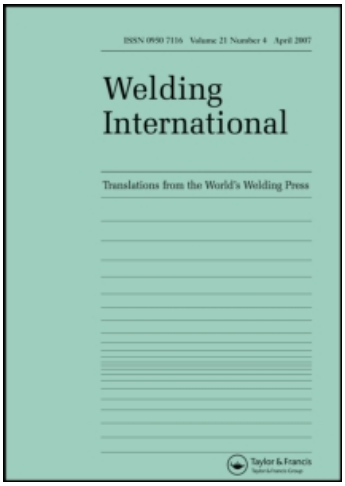

Welding International
Publication details, including instructions for authors and subscription information:
http://www.informaworld.com/smpp/title~content=t778164493

Fluxless laser brazing of aluminium alloy to galvanized steel using a tandem beam - dissimilar laser brazing of aluminium alloy and steels

Kazuyoshi Saida[a]; Haruki Ohnishi[a]; Kazutoshi Nishimoto[a]
[a] Graduate School of Engineering, Osaka University, Osaka, Japan

Online publication date: 09 February 2010

To cite this Article Saida, Kazuyoshi , Ohnishi, Haruki and Nishimoto, Kazutoshi(2010) 'Fluxless laser brazing of aluminium alloy to galvanized steel using a tandem beam - dissimilar laser brazing of aluminium alloy and steels', Welding International, 24: 3, 161 — 168
To link to this Article: DOI: 10.1080/09507110902843065
URL: http://dx.doi.org/10.1080/09507110902843065

Welding International
Vol. 24, No. 3, March 2010, 161–168
Selected from *Quarterly Journal of the Japan Welding Society* 2008 26(3) 235–241

Fluxless laser brazing of aluminium alloy to galvanized steel using a tandem beam – dissimilar laser brazing of aluminium alloy and steels

Kazuyoshi Saida, Haruki Ohnishi and Kazutoshi Nishimoto

Graduate School of Engineering, Osaka University, Osaka, Japan

(*Received 28 July 2008*; *final version received 12 September 2008*)

Tandem beam brazing with aluminium filler metal (BA4047) was conducted in order to develop the fluxless laser brazing technique of aluminium alloy (AA6022) to galvanized steels (GA and GI steels). Laser powers of tandem beam and offset distance of preheating beam from the root to the steel base metal were varied. Sound braze beads could be obtained by optimizing the preheating and main beam powers under the offset distances of 0–1 mm. A small amount of zinc remained at the braze interface between galvanized steels and the braze metal. The reaction layer consisting of Fe–Al intermetallic compounds was also formed at the steel interface, and the thickness of reaction layer could be predicted during the laser brazing (thermal cycle) process based on the growth kinetics with the additivity rule. The metal flow analysis of the melted filler metal on joints revealed that wettability and spreadability of the filler metal on the GI steel joint were superior to those on the GA steel joint. The fracture strength of the lap joint attained approx. 55–75% of the base metal strength of aluminium alloy. It was concluded that fluxless laser brazing could be successfully performed by using a tandem beam because the zinc coat layer acted as the brazing flux.

Keywords: aluminium alloy; galvanized steel; fluxless brazing; interfacial reaction; growth kinetics; contact angle; metal flow analysis; joint properties

1. Introduction

Since aluminium not only has good corrosion resistance due to a dense and stable oxide film on its surface, but is also relatively strong and has good workability and recyclability, it is being used in an increasingly wide range of applications. In particular, reduction in the weight of transport vehicles has become an important part of efforts to preserve the global environment, with the use of aluminium in motor vehicles being a focus of particular interest. This use inevitably involves techniques of joining aluminium to steel, the principle structural material for motor vehicles. However, if conventional fusion welding techniques are used to join dissimilar metals such as steel and aluminium, there are problems such as the formation of brittle intermetallic compounds at the joint interface and a marked decrease in joint strength so there is need for a joining technique that can ensure high reliability.

Brazing is one example of a simple and high-quality joining process capable of being used for aluminium and steel. It is anticipated that the production of brittle intermetallic compounds can be inhibited through the use of filler metals with low melting points. Oven brazing, however, still has residual problems with control of brazing quality and the assurance of high quality. Problems associated with torch brazing include the need for high levels of technical skill. In recent years the technique of laser brazing[1,2], in which a laser is used as the heat source, has attracted attention as a new technique that offers the prospect of solving these problems. In particular, the semiconductor laser (HD laser), since it has a short wavelength with a high absorption rate into metals, has great possibilities for use in brazing[3–5].

The present authors have previously reported that it is possible to carry out good laser brazing of aluminium alloy and steel using a high-power semiconductor laser[6,7]. It was noted that the use of a brazing flux (Nocolok brazing flux) was unavoidable to obtain excellent joint characteristics. However, the use of flux involves the application of a flux coating before brazing and the removal of residual flux after brazing, which tends to reduce work efficiency and productivity. In this study, lap brazing was performed using a tandem beam and the bead formation and the joint characteristics studied, with the aim of developing a fluxless laser brazing method of aluminium alloy and galvanized steel.

2. Specimens and test methods

2.1 Specimens

The base metals of the specimens were the aluminium alloy AA6022 and two types of galvanized steel (alloyed galvanized steel GA, SCGA270 and hot-dip galvanized steel GI, GI70), and Al–12mass%Si alloy (BA4047) aluminium flux was used as the filler metal. The chemical compositions of these are shown in Table 1. The aluminium alloy sheets were 1.2 mm thick and galvanized steel sheets

ISSN 0950-7116 print/ISSN 1754-2138 online

DOI: 10.1080/09507110902843065
http://www.informaworld.com

Table 1. Chemical compositions of materials used (mass%).

(a) *Aluminum alloy and filler metal*								
Alloy	Si	Fe	Mn	Mg	Cr	Zn	Ti	Al
AA6022	1.00	0.15	0.07	0.56	0.02	0.01	0.02	Bal.
BA4047	12.0	0.20	0.01	0.01	–	–	–	Bal.
(b) *Galvanized steels*								
Galvanized steel	C	Si	Mn	P	S	Fe		
SCGA270 (Zinc coat)	0.01	0.01	0.16	0.13	0.06	Bal.		
	(Fe, 9–11; Al, 0.2–0.3; Zn, Bal.)							
GI70 (Zinc coat)	0.01	0.10	0.83	0.10	0.06	Bal.		
	(Fe, 1–2; Al, 0.1–0.2; Zn, Bal.)							

were 0.8 mm thick and the filler metal wire was 1.2 mm in diameter.

2.2 Test methods

The method of tandem beam laser brazing is shown in Figure 1. The aluminium alloy was placed on top of the galvanized steel, the entirety was placed at an angle of 15° and laser brazing was applied to the lap weld part. A preheating beam (rated power, 500 W) and a main beam (rated power, 2 kW) were used for the tandem beam and the power of both the laser beams and the position of the preheating beam irradiation were varied (see Figure 1(b)) for the offset distance from the lap route part of the galvanized sheet side. The laser brazing conditions are shown in Table 2. No flux was used.

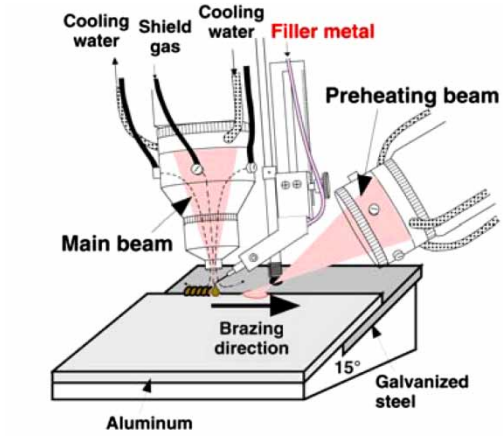

(a) Tandem beam brazing of lap joint

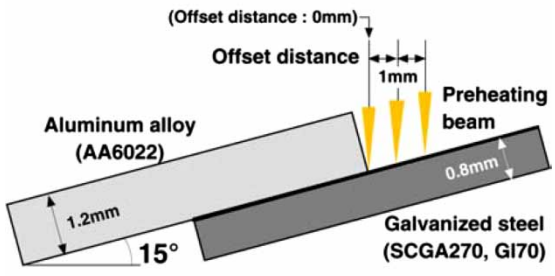

(b) Irradiation position of preheating beam

Figure 1. Schematic illustrations of tandem beam laser brazing procedures.

Inspection of the microstructure of the brazed part and elementary analysis were carried out by optical microscope, scanning electron microscopy and electron probe micro analysis (EPMA). In order to elucidate the production of the brazing interface reaction layer, the galvanized steel was immersed for 2–30 s in molten filler metal bath (test temperature, 923–1023 K), and the thickness of the reaction layer formed at the interface was measured. The interface reaction phase was identified by X-ray diffraction analysis (specific X-ray, Co Kα, tube voltage 50 kV, and tube current 30 mA).

The temperature of the molten brazed layer during the laser brazing process and the temperature distribution of the base metal due to the preheating beam were measured by thermocouples attached at various locations on the joint base metals[8]. The wetting properties (contact angle) of the molten filler metal to the galvanized steel were measured by the sessile drop method and by a similar growing melt drop method[9].

On the other hand, the mechanical properties of the brazed joint were evaluated by a normal temperature tensile shear test with specimens as shown in Figure 2. The joint strength was a value obtained by dividing the failure load by the specimen width. The tension speed was 1.0 mm/min.

Table 2. Laser brazing conditions.

Processing parameter	Value
Main beam power (W)	800–1100
Preheating beam power (W)	0–450
Defocusing distance of main beam (mm)	0
Defocusing distance of preheating beam (mm)	0
Offset distance of preheating beam (mm)	0–2
Distance between beams (mm)	3
Travelling velocity, V_w (mm/s)	5
Wire feeding speed, V_f (mm/s)	10
Wire speed position	Just on surface
Angle of incidence of preheating beam (°)	50
Ar gas flow rate (l/min)	15

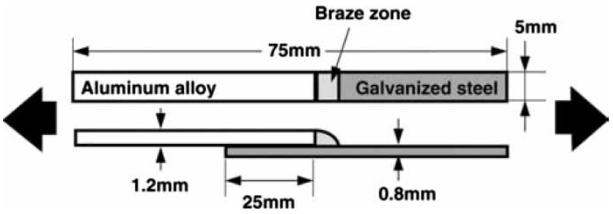

Figure 2. Dimensions of specimen for tensile shear test.

3. Formation properties of the braze bead

Figure 3 shows the results of an investigation of the effects of the preheating beam position on the bead forming properties of the GA steel joint. A good bead was obtained with all preheating beam positions, and at the 2 mm preheating beam offset position the bead width tended to a little smaller than when the preheating beam was at a 0–1 mm offset position. It was also noted that the bead wetting and spreading properties were reduced at 200 W compared to 100 W. Figure 4 shows the effects of preheating beam power on the formation of the braze bead on GA and GI steel joints (with a main beam power of 1000 W). With a preheating beam power in the range 50–100 W, a consistent and good bead form was observed. It is clear that the wetting and spreading qualities of the filler metal on a GI joint were far better than with a GA joint. The effect of the preheating beam power on the toe angle (wetting) of the reinforcement of the braze bead is shown in Figure 5. As the preheating beam power increases, the toe angle of the reinforcement decreases but in GA steel joints, some conditions were noted in which, conversely, the toe angle of the reinforcement increases as the preheating beam power increases. It is thought that this is because the molten zinc alloys with the steel base metal, and the wetting properties decrease, due to excessive preheating. If the preheating beam power is greatly

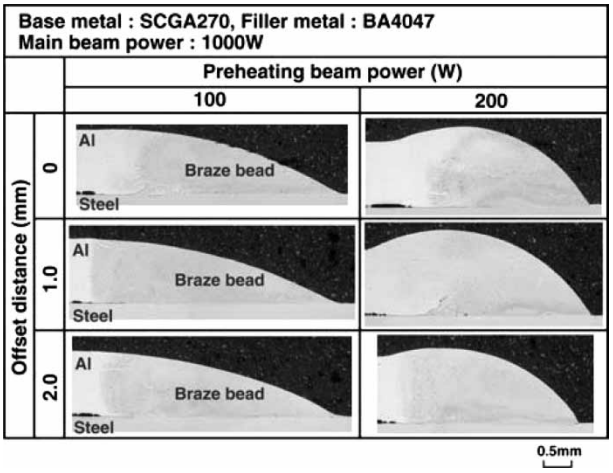

Figure 3. Effects of laser power and offset distance of preheating beam on formation of braze bead in GA steel joint.

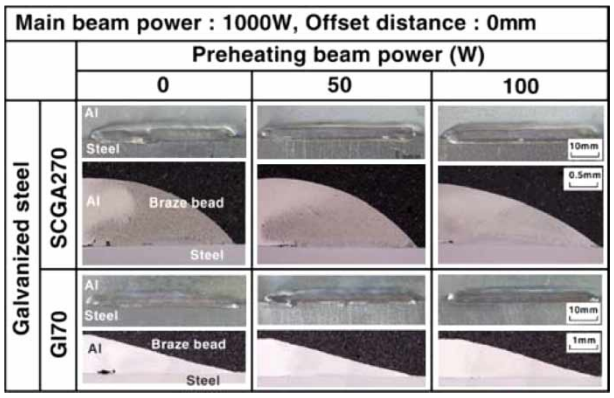

Figure 4. Effect of preheating beam power on formation of braze bead in GA and GI steel joints.

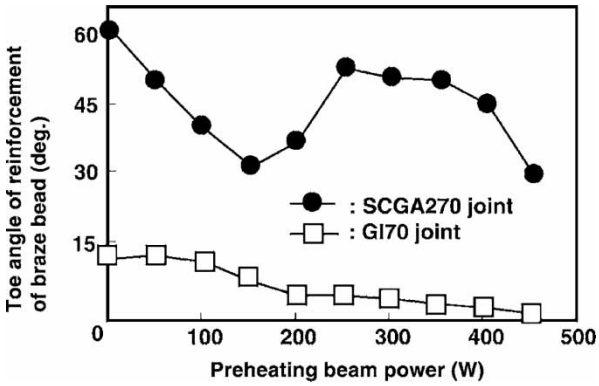

Figure 5. Effect of preheating beam power on toe angle of reinforcement of braze bead at steel substrate in GA and GI steel joints.

increased, the wetting properties once again increases, possibly because the zinc plating layer alloyed with the base metal is fused again. Thus, the wetting of the galvanized steel by the filler metal is generally good and, if appropriate preheating is used, it is possible to assure the shape of the braze bead without the use of flux.

4. Microstructure analysis and interface reaction behaviour of the braze

4.1 Microstructure analysis of the braze

The braze zone microstructure of an AA6022/GA steel weld is shown in Figure 6. A dendrite microstructure is observed at the AA6022/filler layer interface. On the other hand, the surface of the GA steel/filler layer interface is straight and it was thought that there was no obvious erosion and a 2–3 μm production phase (interface reaction layer) was observed at the braze interface in the microstructure. Analysis of the element distribution at the GA steel/filler layer interface is shown in Figure 7. It is clear that aluminium and silicon are present eutectically

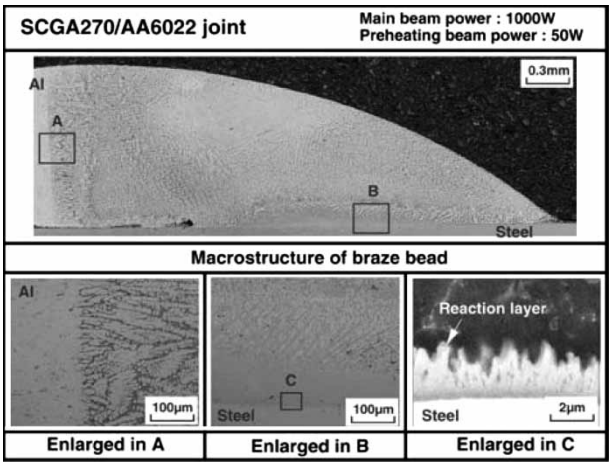

Figure 6. Macro and microstructures of braze zone in GA steel joint (offset distance, 0 mm).

within the filler layer and that iron and aluminium are concentrated at the interface reaction layer. As a result of the identification of the production phase of this GA steel/filler layer interface by X-ray diffraction, it was found that this consisted of Fe–Al intermetallic compounds (Fe_2Al_5 and $FeAl_3$; Figure 8). On the other hand, since only a very small quantity of residual zinc was noted at the steel interface surface (Figure 7), it was thought that the zinc plating layer has played the role of flux (that is, the zinc plating layer has been melted by the preheating beam

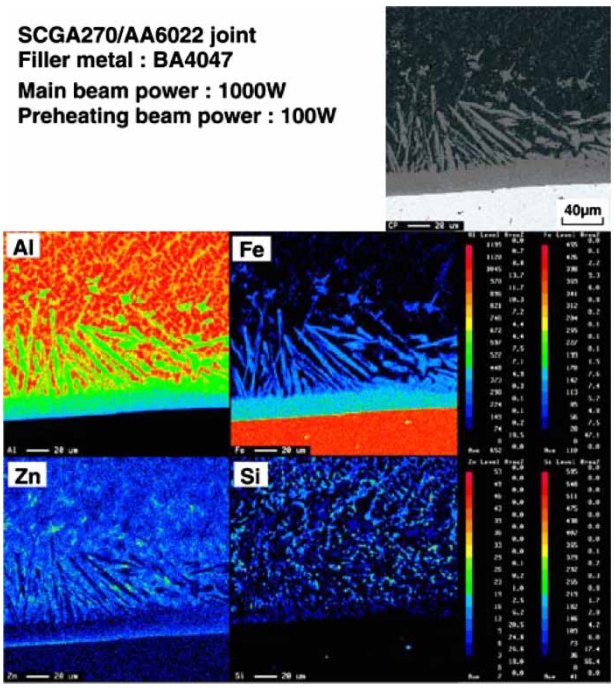

Figure 7. Element distribution in braze zone of GA steel joint analyzed by EPMA (offset distance, 0 mm).

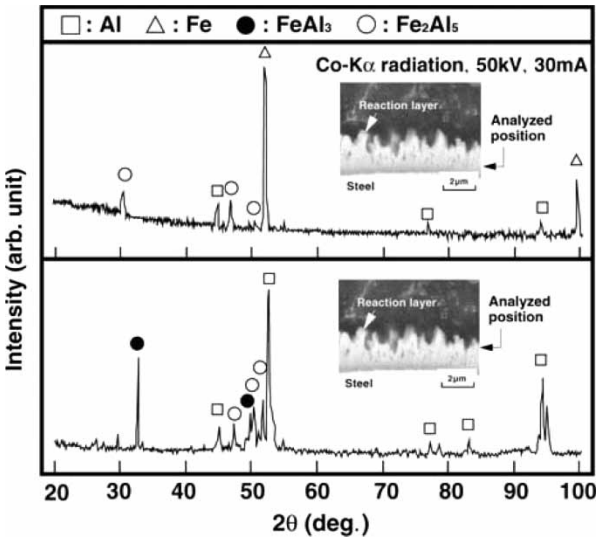

Figure 8. X-ray diffraction patterns of reaction layer at steel/braze metal interface in GA steel joint (offset distance, 0 mm).

and the molten brazing material has wetted the upper steel surface covered by the molten metal), assuring the brazing properties. The formation of a similar microstructure, elementary distribution and an interface reaction layer is also noted in the area of the AA6022/GI steel brazing zone.

4.2 Production behaviour of the interface reaction layer

The changes in the thickness of the interface reaction layer due to isotemperature immersion treatment in which the galvanized steel is immersed in molten filler metal was investigated in order to discover the formation behaviour of the interface reaction layer at the GI steel/filler layer interface surface. Figure 9 shows the relationship between the reaction layer thickness at the GI steel/molten filler metal interface and the square root of the holding time (immersion time). It was confirmed that the interface reaction phase produced in these tests is similar to the interface reaction phase produced by laser brazing. The higher the temperature and the longer the time of this treatment, the thicker is the interface reaction layer. Since a linear relationship was noted between the reaction layer thickness at the interface and the square root of the holding time at all process temperatures, it is clear that the interface reaction layer grows according to the parabolic growth law. Calculation of the apparent activation energy Q and vibration factor k_0 from an Arrhenius plot of the reaction layer growth rate constant (the slope of the line) determined that $Q = 42.0\,\text{kJ/mol}$ and $k_0 = 221.4\,\mu\text{m/s}^{1/2}$.

The interface reaction layer thickness was calculated using the additivity rule, based on the thermal cycle of the

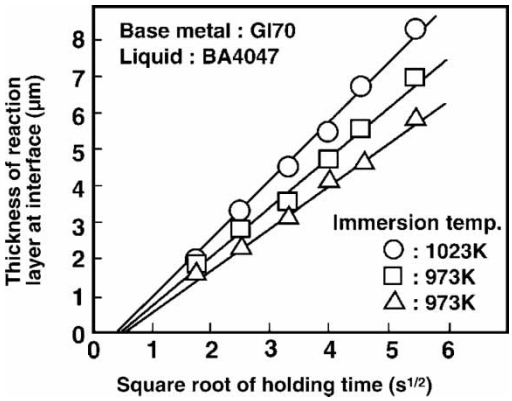

Figure 9. Relation between reaction layer thickness at GI steel/molten BA4047 interface and square root of immersion time (holding time).

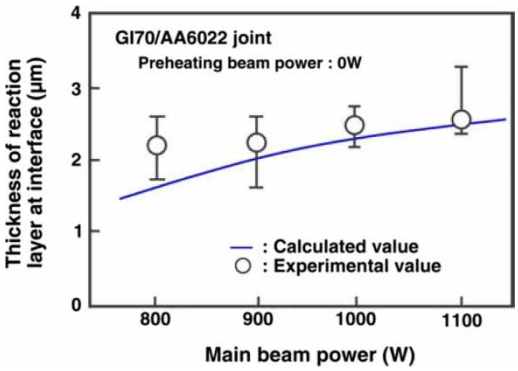

Figure 10. Comparison of reaction layer thickness at GI steel/braze metal interface in laser-brazed joint between calculated results and experimental ones.

molten filler layer measured during the laser brazing process with the main beam power varied. The results are shown in Figure 10. As the main beam power increases, the interface reaction layer thickness increases uniformly. Since the calculated value and experimental values for the interface reaction layer thickness almost completely matched, it is clear that it is possible to predict the formation of the interface reaction layer during the laser brazing process.

5. Analysis of the wetting and flow behaviour of the molten filler metal

5.1 Analytical methods and analytical models

The wetting and flowing behaviour of molten filler metal during the process of laser brazing of aluminium alloy and galvanized steel was analysed[10] using FLOW-3D, a flow analysis software package. Figure 11 gives the analysis models. A lap joint of aluminium alloy and galvanized steel (incline angle, 15°) was simulated, with a model of a

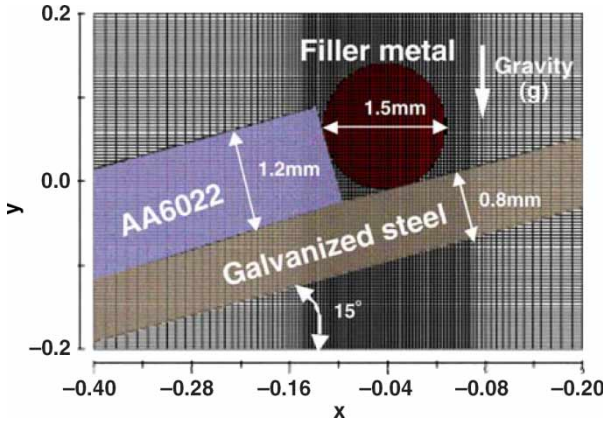

Figure 11. Analyzed models for wetting and spreading of braze metal in laser brazing of AA6022 to galvanized steels.

1.5 mm diameter filler metal (assuming that the filler feed rate/laser scan rate = 10/5) applied to both base metals, 0.8 mm galvanized steel and 1.2 mm aluminium alloy, and the effect of the main beam conditions was given by the initial temperature of molten filler metal droplets (experimental value, 1245 K, when the main beam power is 1000 W) and the effect of the preheating beam condition was given by the experimental temperature distribution for the base metal (Figure 12). The material constants used in the analysis are shown in Table 3. As far as possible, values for the base metal composition[11–16] were used as the material constants but some of the material constants (viscosity, thermal conductivity and surface tension) were values for pure aluminium and pure iron. The equilibrium contact angles on the galvanized steel were measured by the growing melt drop method, as shown in Figure 13. As shown in the figure, the fact that the molten filler metal did not wet the steel that was not zinc plated, supports the supposition that the zinc plating plays the role of flux.

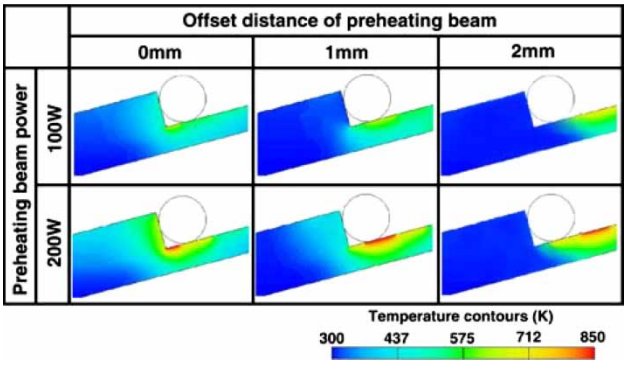

Figure 12. Preheating temperature distribution used for computer simulation.

Table 3. Materials constants of base and filler metals used for metal flow simulation.

(a) *Filler metal*		
Filler metal	BA4047	
Density (g/cm^3)	2.38	
Viscosity (MPa s)	$0.244\exp(1884.7/T)$	
Thermal conductivity (erg/s cm K)	2.37×10^7	
Surface tension (dyn/cm)	$-0.1968T + 1049.6$	
Liquid temperature (K)	868	
Solid temperature (K)	851	
Specific heat (erg/g K)	9.0×10^6	
Latent heat of fusion (erg/g)	3.999×10^9	
(b) *Base metal*		
Base metal	Aluminium alloy (AA6022)	Galvanized steel (SCGA270, GI70)
Density (g/cm^3)	2.7	7.86
Thermal conductivity (erg/s cm K)	1.8×10^7	0.802×10^7
Specific heat (erg/g K)	9.0×10^6	4.4×10^6
(c) *Contact angle of molten filler metal BA4047 on galvanized steels (measured)*		
Basal metal	Contact angle (°)	
SCGA270 (fluxless)	65	
GI70 (fluxless)	2	

T, temperature (K).

5.2 *Analysis results*

The results of the analysis of the melting and spreading behaviour of molten filler metal with varying preheat beam power and irradiation position on GA joints are shown in Figure 14 (main beam power, 1000 W). Within the scope of this study, even when the preheat beam power and irradiation position were varied, no major difference in wetting and spreading characteristics of the molten filler metal was observed, but when the offset distance of the preheat beam irradiation was 2 mm, there was an observable tendency for the wetting and spreading to be reduced. Figure 15 gives the comparison of wetting and spreading profiles of molten metal filler on GI steel joints and GA steel joints (main beam power, 1000 W). GI steel joints showed exceedingly better wetting and spreading characteristics than GA steel joints at all positions of the preheat beam irradiation. These analysis results match well with the experimental results shown in Figure 4 (that the wetting and spreading characteristics of molten filler metal are far better on GI steel joints than GA steel joints), and it was judged that it is possible to predict bead growth behaviour by theoretic analysis.

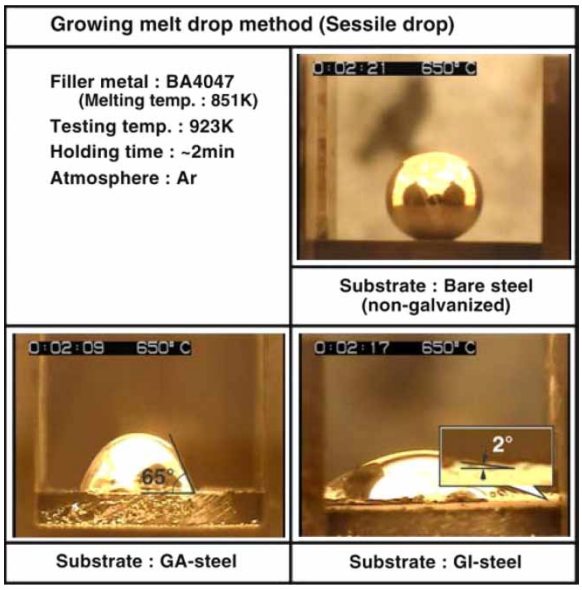

Figure 13. Contact angles of molten filler metal on galvanized steels measured by growing melt drop method.

6. Mechanical properties of laser-brazed joints

The failure strengths of laser-brazed joints of aluminium alloy AA6022 to GA steel or GI steel are shown in Figure 16. This shows that the maximum failure strength of GA steel

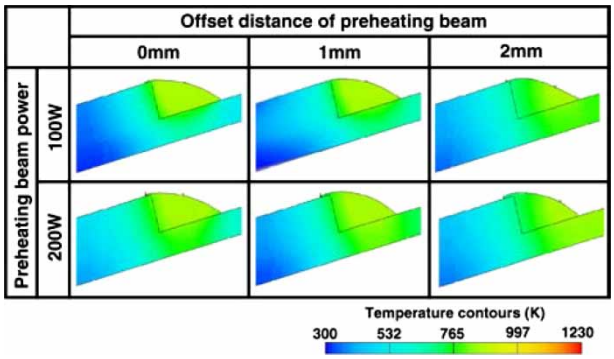

Figure 14. Wetting and spreading profiles of braze metal on GA steel joint with varying laser power and offset distance of preheating beam (main beam power, 1000 W).

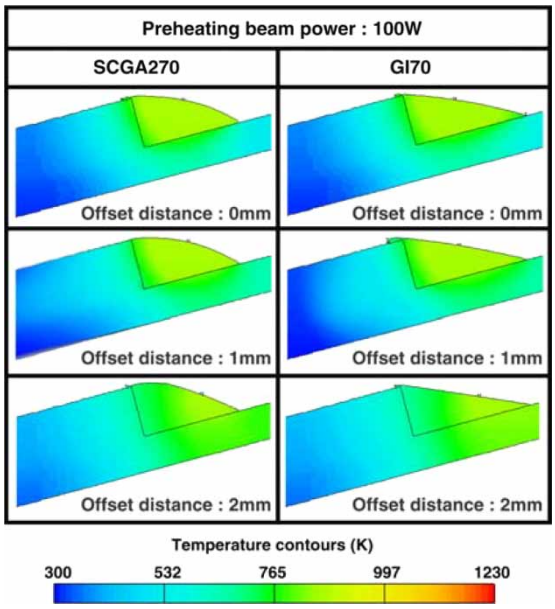

Figure 15. Comparison of wetting and spreading profiles of braze metal between GA and GI steel joints (main beam power, 1000 W).

joints is 130 N/mm, when the main beam power is 800 W and the preheating beam power is 100 W, which is 55% of the strength of the aluminium alloy base metal. It was found, on the other hand, that with a GI steel joint, it reached 180 N/mm, 75% of the aluminium alloy base metal strength, at a main beam power of 1000 W and a preheating beam power of 200 W. Some of the GA steel joints of the highest strength failed in the filler layer and, apart from these, failures occurred in all joints at the steel/filler layer interface. In all GI steel joints, by contrast, failure occurred in the filler layer. From these findings, it is clear that it is possible to fluxlessly tandem beam braze aluminium alloy and galvanized steel to produce joints with good characteristics.

7. Conclusions

In this study, fluxless laser brazing of aluminium alloy and galvanized steel was carried out and the formation of the braze bead and the braze zone microstructure and mechanical properties were assessed. The results obtained were as follows:

(1) When laser brazing was carried out with varied preheating beam and irradiation conditions, it was possible to obtain good joints when the preheating beam irradiation position was offset in the range 0–1 mm. It was found that the wetting and spreading characteristics of the molten filler metal were far better on the GI steel joint than on the GA steel joint.

(2) When the braze zone microstructure was examined and an elementary analysis carried out, it was found that a reaction layer comprising Fe_2Al_5 and $FeAl_3$ was formed at the galvanized steel/filler layer interface and that zinc remained at some parts of the steel interface.

(3) It was found that the intermetallic compounds produced at the steel/molten filler metal interface surface grow according to the parabolic growth law. When the intermetallic compound layer thickness was approximately calculated according to the additivity rule, based on the temperature measurements of the molten filler metal layer during the laser brazing process, the calculated and experimental values matched well and it was possible to make a semi-quantitative prediction of the quantity of the intermetallic compounds formed at the braze interface.

(4) When the wetting and spreading behaviour of the molten filler metal on the aluminium alloy/galvanized steel lap joint were analysed, it was found that the wetting and spreading characteristics on GI steel joints were superior to those on GA steel joints and that the analysis results and experimental results matched closely.

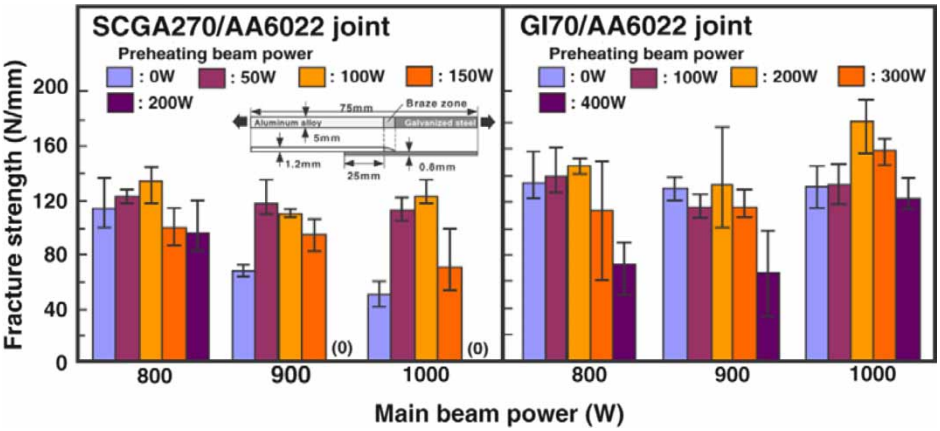

Figure 16. Joint strength of fluxless laser-brazed joints of AA6022 to galvanized steels.

(5) When the mechanical properties of the laser-brazed joints were assessed, it was found that the maximum failure strength of GA steel joints was 130 N/mm, 55% of the strength of the aluminium base metal. On the other hand, the maximum failure strength of GI steel joints was 180 N/mm, 75% of the strength of the aluminium base metal.

Acknowledgements

We would like to express our sincere gratitude to Toyota Motors for their kind assistance during this study.

References

1. Gao YP, Seaman RF, McQuillan TJ. Laser brazing of high temperature braze alloy. IIW Doc. IA-1054-2001.
2. Gao YP, Seaman RF, McQuillan TJ, Martiens RF. Diode laser brazing of space shuttle main engine nozzle. IIW Doc. IA-1056-2001.
3. Saida K, Nishimoto K. Development of LD laser brazing/braze repair welding techniques of Inconel 600 using heat-resisting precious metal fillers. Bureizu (Braze). 2002;36(107):22–33 (in Japanese).
4. Song W, Saida K, Hiramatsu N, Nishimoto K, Shirai M. Brazability of Inconel 600 alloy by a diode laser with heat-resisting precious filler metals, study on laser brazing using high power diode laser beam (report 1). Q J Jpn Weld Soc. 2005;23(4):587–594 (in Japanese).
5. Saida K, Song W, Nishimoto K. Laser brazing of alloy 600 with precious filler metals. Sci Technol Weld Join. 2006;11(5):694–700.
6. Song W, Saida K, Ando A, Nishimoto K. Brazability of aluminum alloy to steels using aluminum filler metal – dissimilar laser brazing of aluminum alloy and steels (report 1). Q J Jpn Weld Soc. 2004;22(2):315–322 (in Japanese).
7. Saida K, Song W, Nishimoto K. Diode laser brazing of aluminum alloy to steels with aluminum filler metals. Sci Technol Weld Join. 2005;10(2):227–235.
8. Saida K, Song W, Nishimoto K. Computer simulation of wetting and flowing behaviors of filler metal during laser brazing process – advanced welding and micro joining/packaging for the 21st century. Mater Sci Forum. 2008;580(582):271–274.
9. Nagashima T, Katoh H, Saita Y, Satoh T, Kinoshita K. Wettability and surface tension of molten InGaAs. J Jpn Soc Microgravity Appl. 1999;16(4):295–299.
10. Saida K, Song W, Nishimoto K. Theoretical approaches to erosion and wetting phenomena during laser brazing process, designing of interfacial structures in advanced materials and their joints. Solid State Phenom B Diffus Defects Data. 2007;127:301–306.
11. Hatano S. Industrial materials handbook. Tokyo: The Nikkan Kogyo Shinbun Ltd; 1981 (in Japanese).
12. Japanese Stainless Steel Association. Stainless steel handbook. Tokyo: The Nikkan Kogyo Shinbun Ltd; 1995 (in Japanese).
13. Arens MF, Acoff VL, Reddy RG. Physical properties of selected filler metals. Sci Technol Weld Join. 2004;9(5):423–429.
14. Kasama A, Iida T, Morita Z. Temperature dependence of surface tension of liquid pure metals. J JIM. 1976;40(10):1030–1038 (in Japanese).
15. Hirai M. Estimation of viscosities of liquid alloys. ISIJ Int. 1993;33(2):251–258.
16. Morioka S. Evaluation of the viscosity for binary and ternary liquid alloys. Mater Sci Eng. 2003;A362:223–227.